

Cloud Liquid Content Retrieval Errors Related to the Flat-layered Cloudfield Model Usage

D. P. Egorov¹, Ya. A. Ilyushin^{1,2}, B. G. Kutuza¹, and Ya. V. Koptsov²

¹Kotel'nikov Institute of Radio Engineering and Electronics of RAS, Russia

²Moscow State University, Faculty of Physics, Russia

Abstract— A problem of atmospheric moisture content distribution retrieval by means of dual-frequency radiometric method is considered. Systematic errors in cloud liquid water content retrieval related to the use of a homogeneous flat-layered cloudfield model, which ignores discontinuous and inhomogeneous structure of real cloudiness, are being investigated. To estimate these errors, a simulation of microwave spatial field of brightness temperature of the “ocean–atmosphere” system with discontinuous cumulus cloudiness taken into account is performed on the basis of Planck’s model for random cloud fields generation, the standard atmosphere model, and the smooth water surface reflection model. An extensive database of simulated brightness temperature 2D-distributions has been precomputed for different values of Planck’s model parameters. Fast software algorithms have been developed to process the data. That makes it possible to analyze mentioned systematic errors comprehensively for various initial cloud cover percentage while changing the size of antenna’s resolution (or averaging) element by means of which a picture of discontinuous cloudiness is being reduced to a set of plane-layered approximations. The dependencies obtained are presented for various pairs of frequencies used in dual-frequency method and may be approximated, for example, by polynomials. The numerical simulation shows that for any Planck’s distribution with a given cloud cover percentage the relative error of area-averaged liquid water content retrieval grows when the resolution element of antenna increases in size. It also shows that for any fixed size of the resolution element, if clouds are distributed in accordance to Planck’s model, a decrease of cloud cover percentage (while all the other model parameters stay the same) leads to an increase in the relative error of area-averaged liquid water content retrieval.

1. INTRODUCTION

The microwave radiometric method makes it possible to evaluate such integral moisture content parameters as total water vapor mass in atmosphere and liquid water content (LWC) in clouds by processing the data on brightness temperatures obtained at various frequencies [1–4]. In ground-based observations of downwelling radiation, the size of microwave radiometer’s spatial resolution element is usually much smaller than the size of a cloud. That makes it possible to study the spatio-temporal variability of the atmospheric moisture content field [5, 6, 7]. At the same time, the spatial resolution of modern satellite microwave radiometers in 10-40 GHz frequency range is 12-30 kilometers, which is significantly larger than the horizontal extent of many species of clouds, including cumulus ones. When solving the inverse problem of atmospheric moisture content parameters retrieval, as a rule, a homogeneous plane-layered model for a cloud field is usually adopted, which ignores the properties of discontinuous and inhomogeneous structure of real cloudiness. In other words, gaps between clouds, horizontal and vertical extent of each cloud, or at least the corresponding statistical estimates per unit area are not taken into account. This fact, and also the non-linearity of dependence of atmospheric brightness temperature on cloud LWC, leads to systematic errors in aforecited integral parameters retrieval. To estimate these errors arising in case of sounding from space one have to describe several different models. As it seems, these are: a statistical model for whole cloudfield structure, which declares the distribution of clouds by diameter and power closely to usually observed in reality; a model, that describes structure of a separate cloud, specifically its liquid water altitude profile and integral LWC; a model for radiation properties of clouds with certain established features; a radiation model for standard atmosphere with given meteo parameters combined with the previous model; an underlying surface radiation and reflection model. Finally, one have to use certain approach for solving the inverse problem of total water vapor mass and LWC retrieval. Herewith, it is necessary to pay attention to the features of sounding antenna, its resolution.

In this paper, Plank's model [8] is suggested for specifying cloudfield structure (see section 4). Cumulus clouds are under consideration. The statistical dependence of LWC of a separate cumulus cloud on its vertical extent is taken from [1]. Mazin's law [9, 10] is used to estimate the cloud liquid water altitude profile. Radiation model of standard atmosphere but with added cloudiness and smooth water as an underlying surface is described (see section 2). The dual-frequency method for atmospheric integral moisture content distribution retrieval is explained (see section 3). Brief analysis of mentioned systematic errors in area-averaged LWC retrieval is shown (see section 5).

2. RADIATION OF OCEAN-ATMOSPHERE SYSTEM. SMOOTH WATER SURFACE

Brightness temperature of "underlying surface – atmosphere" system outgoing thermal radiation, which is received on vertical or horizontal polarization at a certain frequency ν , zenith angle θ , $0 \leq \theta \leq 0.4\pi$, can be written as (indices ν are omitted for simplicity)

$$T_{v,h}^*(\theta) = T^\uparrow(\theta) + T_s \cdot \kappa_{v,h}(\theta) \cdot e^{-\tau(0) \sec \theta} + T^\downarrow(\theta) \cdot R_{v,h}(\theta) \cdot e^{-\tau(0) \sec \theta}, \quad (1)$$

where atmosphere is assumed to be a multilayered uniform medium,

$$T^\downarrow(\theta) = \int_0^\infty T(h) \gamma(h) \sec \theta \cdot \exp \left[- \int_0^h \gamma(z) \sec \theta dz \right] dh \quad (2)$$

is downwelling atmospheric brightness temperature (the expression for upward radiation $T^\uparrow(\theta)$ differs only in the limits of integration), h is altitude, $\gamma(h)$ is total for all atmospheric components path attenuation coefficient at this altitude, $T(h)$ represents atmospheric thermodynamic temperature profile, $\tau(0)$ is total zenith ($\theta = 0^\circ$) opacity equal to the integral of the attenuation coefficient $\gamma(h)$ for h from zero to infinity; $R_{v,h}(\theta)$ is surface reflectance (depending on polarization), $\kappa_{v,h}(\theta)$ is emissivity of this surface ($\kappa_{v,h}(\theta) = 1 - R_{v,h}(\theta)$ under the assumption of local thermodynamic equilibrium), and T_s denotes its thermodynamic temperature. Cosmic background radiation temperature is not taken into account here.

For smooth water surface [1, 11], the coefficient of reflectance $R_{v,h}(\theta)$ can be expressed in terms of complex dielectric permittivity ε of water. After introducing a sliding angle $\psi = 90^\circ - \theta$

$$R_{v,h}(\theta) = R_{v,h}(90^\circ - \psi) = |M_{v,h}(\psi)|^2, \quad (3)$$

where

$$M_h(\psi) = \left[\sin \psi - (\varepsilon - \cos^2 \psi)^{0.5} \right] \cdot \left[\sin \psi + (\varepsilon - \cos^2 \psi)^{0.5} \right]^{-1}, \quad (4)$$

$$M_v(\psi) = \left[\varepsilon \sin \psi - (\varepsilon - \cos^2 \psi)^{0.5} \right] \cdot \left[\varepsilon \sin \psi + (\varepsilon - \cos^2 \psi)^{0.5} \right]^{-1}. \quad (5)$$

If $\theta = 0^\circ$, then obviously $\psi = 90^\circ$ and (4), (5) might be reduced

$$M_h = M_v = (\varepsilon^{0.5} - 1) \cdot (\varepsilon^{0.5} + 1)^{-1}. \quad (6)$$

The dielectric permittivity ε depends on radiation frequency ν or wavelength λ and thermodynamic temperature t of water ($t = T_s$ for water surface). In addition, it can be represented as

$$\varepsilon = \left(\varepsilon_O + \frac{\varepsilon_S - \varepsilon_O}{1 + \Delta\lambda^2} \right) - i \cdot \Delta\lambda \cdot \frac{\varepsilon_S - \varepsilon_O}{1 + \Delta\lambda^2}, \quad \Delta\lambda = \frac{\lambda_S}{\lambda}. \quad (7)$$

Here ε_O is "optical" component of dielectric constant, $\varepsilon_S = \varepsilon_S(t)$ is "static" component and $\lambda_S = \lambda_S(t)$ is characteristic wavelength related to water molecules relaxation time. The temperature dependencies for ε_O , ε_S and λ_S parameters can be found in [1, 2, 12]. Corrections for non-zero salinity of water are also given there.

Back to the atmosphere, the total path attenuation coefficient $\gamma(h)$ can be decomposed into the sum of attenuations for each atmospheric component

$$\gamma(\nu, h) = \gamma_O^*(\nu, h) + \gamma_\rho^*(\nu, h) + \gamma_w^*(\nu, h), \quad (8)$$

where ν is radiation frequency, γ_O^* and γ_ρ^* are path attenuation coefficients for oxygen and water vapor respectively, and γ_w^* is cloud path attenuation (if clouds take place). The first two coefficients can be approximated by theoretical-empirical dependencies $\gamma_O(\nu, h) = \gamma_O(\nu, T(h), P(h))$ (dB/km) and $\gamma_\rho(\nu, h) = \gamma_\rho(\nu, T(h), P(h), \rho(h))$ (dB/km) taken from International Telecommunication Union (ITU) recommendations [13]. Here $P(h)$ and $\rho(h)$ represent atmospheric pressure and absolute humidity altitude profiles, and $T(h)$ is thermodynamic temperature profile as mentioned above. In this case, $\gamma_O^* = \chi \cdot \gamma_O$ and $\gamma_\rho^* = \chi \cdot \gamma_\rho$, where $\chi = 0.23255814$ is conversion factor from decibels (dB) to nepers (np).

The cloud path attenuation γ_w^* can be also expressed in terms of the dielectric permittivity ε of water (particles of cloud formation). Let us introduce a weight function $k_w = k_w(\lambda, t_w)$ as [1]

$$k_w(\lambda, t_w) = \frac{0.6\pi}{\lambda} \cdot K_C, \quad K_C = \text{Im} \left(\frac{\varepsilon - 1}{\varepsilon + 2} \right) = \frac{3 \cdot (\varepsilon_S - \varepsilon_O) \Delta \lambda}{(\varepsilon_S + 2)^2 + (\varepsilon_O + 2)^2 \Delta \lambda^2}. \quad (9)$$

Here λ is wavelength, t_w is an estimation of average effective cloud temperature. The dielectric permittivity ε with its components (7) are computed here for the specified λ and thermodynamic temperature of water t equal to t_w . Finally, the absorption coefficient $\gamma_w^*(\nu, h)$ (np) is simply a product of $k_w^*(\nu, t_w) = k_w(c \cdot \nu^{-1}, t_w)$ weight function and $w(h)$ liquid water amount at h altitude.

The authors have combined (1)-(10) into a single model, which considers the “underlying smooth water surface – atmosphere” system brightness temperature T^* as a function

$$T^* = T^*(\nu, \theta, T_s, t_w, T(h), P(h), \rho(h), w(h), \xi) \quad (10)$$

where $w(h)$ is liquid water altitude profile, ξ denotes chosen polarization (horizontal or vertical) and all other designations are listed in the text above. This model has been implemented in software.

3. ATMOSPHERIC MOISTURE CONTENT PARAMETERS RETRIEVAL

The dual-frequency radiometric method for integral moisture content parameters retrieval is presented in [1–4]. It allows to evaluate the values of total water vapor mass Q (g/cm²) and cloud liquid water content W (kg/m²) based on the brightness temperatures registered. If cloud effective temperature t_w is estimated, moreover, the total atmospheric opacity is relatively small $\tau \lesssim 1$ np, then it is sufficient to solve a system (11) of two linear equations written down for two different frequencies ν_1, ν_2 by any available method to get the integral parameters

$$\tau_{\nu_i} = \tau_O(\nu_i) + k_\rho(\nu_i) \cdot Q + k_w^*(\nu_i, t_w) \cdot W, \quad i = 1, 2, \quad (11)$$

where τ_ν is an estimation of atmospheric total zenith opacity (np), $\tau_O(\nu)$ is model value of zenith opacity in oxygen (np), $k_w^*(\nu, t_w)$ is the previously considered (see (9)) weight function for attenuation in clouds, and an expression for $k_\rho(\nu)$ weight function can be written e.g. as follows

$$k_\rho(\nu) = \gamma_\rho^*(\nu, 0) \cdot H^\nu \cdot \left(\int_0^\infty \rho(h) dh \right)^{-1}. \quad (12)$$

Here $\gamma_\rho^*(\nu, 0) = \gamma_\rho^*(\nu, T(0), P(0), \rho(0))$ is the path attenuation coefficient (np/km) related to water vapor and computed at zero altitude level (see (8)), H^ν is the characteristic height of attenuation in water vapor (from 1.6 to 2.1 km), and $\rho(h)$ represents the standard altitude profile of water vapor (absolute humidity).

After the model values of τ_O , k_ρ and k_w are evaluated for both frequencies, the main problem is to retrieve the atmospheric total zenith opacity τ_{ν_i} (or $\tau(0)$ in other designations, when ν is omitted). Let us consider approximations for brightness temperatures of upward $T^\uparrow(\theta)$ and downwelling $T^\downarrow(\theta)$ radiation

$$T^\uparrow(\theta) = T_{av}^\uparrow \left(1 - e^{\tau(0) \sec \theta} \right), \quad T^\downarrow(\theta) = T_{av}^\downarrow \left(1 - e^{\tau(0) \sec \theta} \right), \quad (13)$$

where T_{av}^\uparrow and T_{av}^\downarrow are average effective temperatures for upward and downwelling radiation respectively, $0 \leq \theta \leq 0.4\pi$. Using these approximations, one can rewrite (1) as (14)

$$T_{v,h}^*(\theta) = T_{av}^\uparrow \left[1 - e^{-\tau(\theta)} \right] + T_s \cdot \kappa_{v,h}(\theta) \cdot e^{-\tau(\theta)} + T_{av}^\downarrow \left[1 - e^{-\tau(\theta)} \right] R_{v,h}(\theta) e^{-\tau(\theta)}. \quad (14)$$

Here $\tau(\theta)$ is understood as $\tau(0) \cdot \sec \theta$. Note, that equation (14) is quadratic with respect to $e^{-\tau(\theta)}$. One can solve it for fixed polarization and thus get an estimation on total opacity (15)

$$e^{-\tau(\theta)} = \frac{-b + \sqrt{D}}{2 \cdot a} \quad \text{or} \quad \tau(0) = \ln \left(\frac{2 \cdot a}{-b + \sqrt{D}} \right) \cdot \cos \theta, \quad (15)$$

where $a = T_{av}^\downarrow \cdot R(\theta)$, $b = T_{av}^\uparrow - T_{av}^\downarrow \cdot R(\theta) - T_s \cdot \kappa(\theta)$, and $D = b^2 - 4 \cdot a \cdot (T^*(\theta) - T_{av}^\uparrow)$.

Hence, to estimate the atmospheric total zenith opacity by outgoing radiation of “underlying surface – atmosphere” system it is necessary, at first, to assess the average effective temperatures T_{av}^\uparrow and T_{av}^\downarrow , the surface reflectance $R(\theta)$ and surface temperature T_s . Errors in assessment of these four parameters lead to an error in total zenith opacity and therefore affect the accuracy of Q and W evaluation. In real experiments, the accuracy of these integral parameters retrieval is also influenced by impossibility of exact τ_O and k_ρ values computation due to discrepancy between the standard $T(h)$, $P(h)$ and $\rho(h)$ profiles and the real ones.

4. CLOUDFIELD MODELING

The field of random discontinuous cloudiness (with gaps between clouds) can be generated according to Planck’s model [8] with the corresponding distribution of clouds by diameters and an unambiguous relation between the power of each cloud and its diameter [11]. Based on the results of processing an extensive database of stereoscopic survey at Florida, USA, Planck (1969) proposed following distribution

$$n(D) = K \cdot e^{-\alpha D}, \quad 0 \leq D \leq D_m. \quad (16)$$

Here D is cloud diameter, $n(D)$ is number of clouds of a certain diameter, D_m is the maximum cloud diameter in the ensemble of clouds, K is normalization coefficient and α – parameter, which depends on the time of day and various local climatic conditions.

Cloud power is the difference in altitudes of cloud top and base. The relation between the cloud power and its diameter can be written as

$$H = \eta D \left(\frac{D}{D_m} \right)^\beta, \quad (17)$$

where η and β are the dimensionless parameters (see [8]).

There is a variety of cloud species to be discussed, but we are concerned here with convective clouds of cumulus type in the first place. Average values of effective temperature, integral liquid water content, power and cloud base altitudes for Cu hum/med/cong cloud species are listed in [1]. The liquid water profile of such a cloud can be obtained as follows (Mazin’s model) [10]

$$\tilde{w}(\xi) = \tilde{w}(\xi_0) \frac{\xi^{\mu_0} (1 - \xi)^{\psi_0}}{\xi_0^{\mu_0} (1 - \xi_0)^{\psi_0}} = \frac{W}{H} \cdot \frac{\Gamma(2 + \mu_0 + \psi_0)}{\Gamma(1 + \mu_0) \Gamma(1 + \psi_0)} \xi^{\mu_0} (1 - \xi)^{\psi_0}, \quad (18)$$

where $\xi = h/H$ is the reduced height inside the cloud, H is the power of cloud (km), W is the integral liquid water content (kg/m^2), $\tilde{w}(\xi)$ represents the profile of liquid water inside the cloud (kg/m^3), $\tilde{w}(\xi_0)$ is the maximum value, and ξ_0 is the reduced height at which the maximum value is reached, μ_0 and ψ_0 are the dimensionless parameters. According to [1], the values of these parameters are $\mu_0 = 3.27$, $\psi_0 = 0.67$, $\xi_0 = 0.83$, and the integral liquid water content W on cloud power H dependence can be approximated based on given tabular data as

$$W = 0.132574 \cdot H^{2.30215}. \quad (19)$$

We introduce a computational domain Ω with an area of 50×50 km, 10 km height and a grid of $300 \times 300 \times 500$ nodes, respectively. Let us assume the shape of clouds to be cylindrical, the boundaries not to be intersected, clouds cannot be located one above the other, and generate a field of discontinuous cumulus cloudiness setting the values of model parameters K , D_m , α , β , η and assigning a fixed interval of heights, in which the cloud base can change. The distribution of clouds by diameter can be calculated from (16) by substitution $k \cdot D_m \cdot r^{-1}$ in place of D . Here k is an integer number, $1 \leq k \leq r$, and r is selected in accordance to available detalization of computational grid. For instance, $r = \sqrt{i_*^2 + j_*^2}$, where i_* , j_* are the numbers of grid nodes per

distance in km along the corresponding directions to cover a cloud of D_m diameter. The numerical simulation shows that iterative filling of Ω with clouds in decreasing order of their diameter makes it possible to achieve maximum percentage of cloud cover (projected on $h = 0$ plane) at the level of 60-65% within an acceptable time of searching for suitable random location for each cloud and without using specialized algorithms for optimal packing. However, it is not possible to obtain a larger cloud cover percentage without algorithms for optimal packing.

Having cloud field generated, let us define at each point of zero altitude plane the liquid water altitude profile $w(h)$ in such a way that $w(h) = \tilde{w}((h - H_0)/H)$ (see (18)), if h is inside a cloud with base altitude equal to H_0 and power equal to H , and, on the other hand, $w(h) = 0$, if h is beyond any cloud. Having the liquid water 3D-distribution $w(i, j, h)$ obtained and setting also the standard altitude profiles of $T(h)$, $P(h)$ and $\rho(h)$ at each point of zero altitude plane, substitute them to the author's model (10). Considering $\theta = 0^\circ$ and, for example, $T_s = 15^\circ\text{C}$, $t_w = -2^\circ\text{C}$ make all the related computations at each point to obtain 2D-map (300×300 nodes) of brightness temperature. An example of the obtained 2D-map can be found in [4]. These 2D-maps can be obtained for various states (seeds) of random cloud locations generator. Thus, a database of simulated brightness temperature 2D-distributions of "smooth water surface – cloudy atmosphere" system can be prepared for any fixed set of K , D_m , α , β , η , θ , T_s and t_w values.

5. ERRORS IN AREA-AVERAGED LIQUID WATER CONTENT

To assess the systematic errors in the liquid water content dual-frequency retrieval related to the flat-layered cloud field model usage, which ignores its real discontinuous and inhomogeneous structure, we apply an operation of block averaging (20) with blocks of $n \times n$ nodes for $n = 1, 2, 3 \dots 300$ sequentially to the prepared brightness temperature 2D-arrays and monitor the dynamics of LWC 2D-picture computed in accordance to (11)-(15).

$$\tilde{T}_b^\nu(i, j) = \sum_{k, l} \frac{T_b^\nu(k, l)}{n^2}, \quad (20)$$

where $n \cdot i^* \leq k < n \cdot (i^* + 1)$, $n \cdot j^* \leq l < n \cdot (j^* + 1)$, and $i^* = [i/n]$, $j^* = [j/n]$ (square brackets represent integer division). Thus, blocks do not have intersections and are understood as elements of resolution (or averaging), by means of which a picture of discontinuous cloudiness (T_b^ν) is reduced to a set of plane-layered approximations (\tilde{T}_b^ν). In other words, each separate block simulates an antenna's resolution element.

For LWC picture retrieval by means of dual-frequency method, two maps of brightness temperature at two different frequencies at the same time are needed. Block averaging then has to be applied to these maps in parallel. Each time the LWC 2D-distribution $W(i, j)$ is obtained, we calculate its average value $W_a = \langle W(i, j) \rangle_{i, j}$ (area-averaging). Average values of LWC retrieved at chosen pair of frequencies for various n are to be compared to "real" area-averaged liquid water content W^* , which has been initially set while corresponding cloudfield generation and can be calculated by integrating the $w(i, j, h)$ distribution over h at each point of zero altitude plane and subsequent averaging. Afterall, we introduce the relative error value W_{err} in the standard way

$$W_{err} = \frac{|W^* - W_a|}{W^*} \cdot 100\%. \quad (21)$$

In figure 1 the dependencies of introduced relative error in area-averaged LWC on cloud cover percentage change is shown for different pairs of frequencies used in dual-frequency method and different sizes of averaging blocks (20), $n = 30$ and 150 nodes. Plank's model parameters are $D_m = 3$ km, $\alpha = 1$, $\beta = 0.5$, $\eta = 1$ and K changes from 44 up to 205. The change in K , when all other parameters stay the same, allows one to control the cloud cover percentage. For every fixed set of K , D_m , α , β , η , θ , T_s and t_w values, and thus for every fixed cloud cover percentage, the cloud locations generator has been launched for 100 times each time with different seed. That means, for every set of mentioned parameters fixed we have 100 different 2D-maps (300×300 nodes) of brightness temperature of statistically identical cloudfields, but with different cloud locations. This allows us to draw the corresponding error bars (see fig. 1).

It occurs, that horizontal location of clouds in cloudfields, where they cannot be stacked one on top of the other, does not affect much on the relative error in LWC when the distributions of clouds by diameter and power are statistically similar for each cloudfield. The non-linearity in

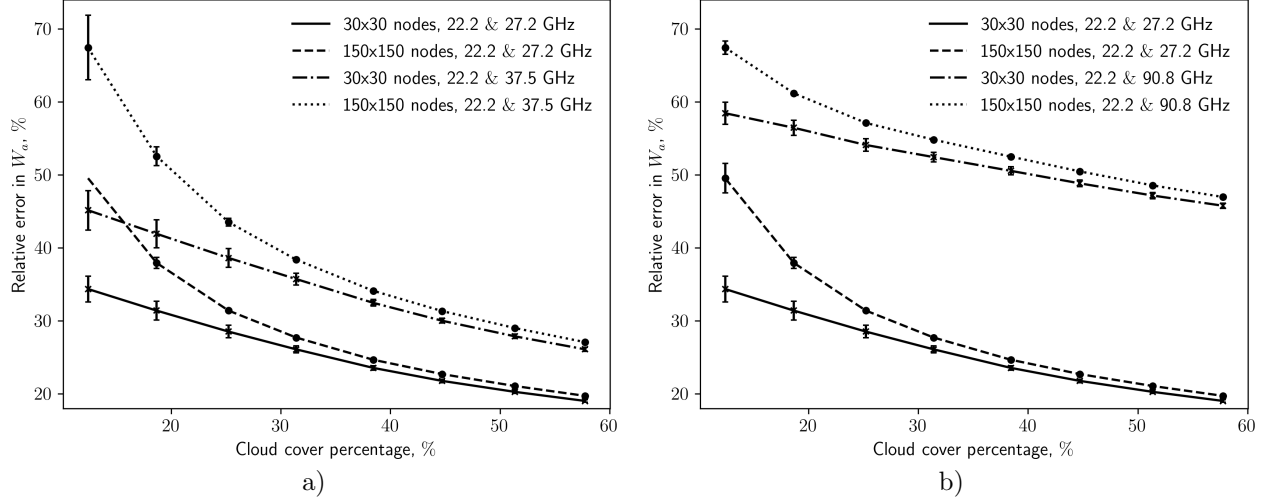


Figure 1: Dependence of the relative error (%) in area-averaged LWC (retrieved by dual-frequency method) on cloud cover percentage. Plank’s model parameters are $D_m = 3$ km, $\alpha = 1$, $\beta = 0.5$, $\eta = 1$ and $K = 44 \dots 205$; $T_s = 15^\circ\text{C}$, $t_w = -2^\circ\text{C}$. The size of resolution element is $n = 30$ or 150 nodes; a) 22.2 and 27.2 GHz frequency pair versus 22.2 and 37.5 GHz pair, b) 22.2 and 27.2 GHz versus 22.2 and 90.8 GHz.

dependence of brightness temperature at certain frequency on cloud LWC (for extremely large or very small values of LWC) and its influence are being researched now and will be presented later. Finally, we can note from figure 1, that for any size of the resolution element and Plank’s cloudfield considered, a decrease of cloud cover percentage (while all the other model parameters stay the same) leads to an increase in the relative error of area-averaged LWC retrieval. It can be also confirmed by numerical simulations, that for any given cloud cover percentage and any chosen pair of frequencies, the relative error of area-averaged LWC dual-frequency retrieval grows when the resolution element of antenna increases in size. We have got very similar results as presented in [4] for cloudy atmosphere downwelling radiation in case of ground-based sounding.

6. CONCLUSION

The spatial 2D-field of outgoing microwave radiation of “smooth water surface – atmosphere” system supplemented with complex cumulus 3D-cloudfield generated in accordance to Plank’s and Mazin’s models has been evaluated for various model parameters. A software for corresponding computations is available on GitHub [14]. Using brightness temperature distributions obtained and simulating the change in size of antenna’s resolution element, an analysis of systematic errors in area-averaged LWC retrieval (from artificial Earth satellites by means of dual-frequency radiometric method) has been partially performed. The authors hope that in continuation of work on this topic it will be possible to develop some recommendations or amendments to the existing approaches of evaluation of atmospheric integral parameters, which are affected by cloudfields discontinuity and inhomogeneity.

The research is carried out using the equipment of the shared research facilities of HPC computing resources at Lomonosov Moscow State University [15]. This work is supported by the State Assignment of Ministry of Science and Higher Education of the Russian Federation theme no. 0030-2019-0008 ”Space”.

REFERENCES

1. Kutuza, B.G., M.V. Danilichev, and O.I. Yakovlev, *Satellite monitoring of the Earth. Microwave radiometry of atmosphere and surface*. LENAND, 2016 (in russian).
2. Basharinov A.E., and Kutuza B.G., “Studies of radiation and absorption of cloud atmosphere in the millimeter and centimeter ranges”, *Proc. Main Geophys. Observatory*, No. 222, 100-110, 1968.
3. Akvilonova A.B., and Kutuza B.G., “Microwave radiation from clouds”, *Sov. J. Commun. Technol. Electron.*, Vol. 23, No. 9, 1792-1806, 1978.
4. Egorov D.P., Ilyushin Ya.A., Koptsov Ya.V. and Kutuza B.G., “Simulation of microwave

- spatial field of atmospheric brightness temperature under discontinuous cumulus cloudiness”, *Journal of Physics: Conference Series* Ser. 1991, 012015, 2021.
5. Egorov D.P., and Kutuza B.G., “Atmospheric Brightness Temperature Fluctuations in the Resonance Absorption Band of Water Vapor 18 - 27.2 GHz”, *IEEE Transactions on Geoscience and Remote Sensing*, Early Access, 1-8, 2020.
 6. Egorov D.P., and Kutuza B.G., “The influence of clouds on atmospheric radiation fluctuations in the resonance absorption band of water vapor 18-27.2 GHz”, *Journal of Physics: Conference Series*, Ser. 1632, 012010, 2020.
 7. Egorov D.P., Kutuza B.G., and Smirnov M.T., “Web portal for a databank of microwave radiometric measurements of the atmosphere in resonant band of water vapor 18-27 GHz”, *Proc. Photon. Electromagn. Res. Symp. Spring (PIERS-Spring)*, Rome, Italy, Jun. 2019, 3421-3427.
 8. Planck V.G., “The size distribution of cumulus clouds in representative Florida populations”, *J. Appl. Met.*, Vol. 8, No. 1, 46-67, 1969.
 9. Mazin I.P., and Shmeter S.M., “Cumulus clouds and the related deformation of fields of meteorological elements”, *Trudy CAO*, No. 134, 53-164, 1977 (in russian).
 10. Voyt F.L., and Mazin I.P., “Water content of cumulus clouds”, *Izv. Akad. Nauk SSSR, Ser. Fiz. Atm. i Okeana*, Vol. 8, No. 11, 1166, 1972.
 11. Kutuza B.G., and Smirnov M.T., “The influence of cloudiness on averaged thermal radiation of ocean surface - atmosphere system”, *Soviet Journal of Remote Sensing*, No. 3, 76-83, 1980.
 12. Rozenberg V.I., *Scattering and attenuation of electromagnetic radiation by atmospheric gases*. St. Petersburg, Russia: Gidrometeoizdat.
 13. Rec. ITU-R P.676-3, Attenuation by atmospheric gases, The ITU Radiocommunication, 1997. url: <https://www.itu.int/rec/R-REC-P.676>
 14. Author’s GitHub-Page, Microwave radiometry of the Earth’s atmosphere, 2021. url: <https://github.com/dobribobri/meteo->
 15. Sadovnichy V., Tikhonravov A., Voevodin V., and Opanasenko, V., “Lomonosov: Supercomputing at Moscow State University”, *Contemporary High Performance Computing: From Petascale toward Exascale. Chapman and Hall/CRC Computational Science*, Boca Raton, United States, 2013, 283-307.